

F FACES OF APATITE AND ITS MORPHOLOGY: THEORY AND OBSERVATION**R.A. TERPSTRA***Institute of Dental Materials Science, University of Nijmegen, P.O. Box 9101, 6500 HB Nijmegen, The Netherlands***P. BENNEMA***Research Institute of Materials, Laboratory of Solid State Chemistry, University of Nijmegen, Toernooiveld, 6525 ED Nijmegen, The Netherlands***P. HARTMAN and C.F. WOENSDREGT***Institute of Earth Sciences, P.O. Box 80021, 3508 TA Utrecht, The Netherlands***W.G. PERDOK***Laboratory of Materia Technica, State University of Groningen, The Netherlands*

and

M.L. SENECHAL*Clark Science Center, Department of Mathematics, Smith College, Northampton, Massachusetts, USA*

Received 8 November 1985; manuscript received in final form 25 July 1986

Eighteen connected nets have been determined for hydroxyapatite, and 12 different F faces run parallel to at least one of these connected nets. The order of morphological importance of these F faces is determined by the slice energy, E_{hkl}^{slice} and compared to the morphological data for natural apatites. It is found that there is a close agreement between predicted and observed morphology. It follows that the lowering of the apatite symmetry ($P6_3/m \rightarrow P2_1/b$) due to the ordering of OH is not likely to be the cause of the occurrence of plate like apatitic crystals in calcified tissues.

1. Introduction*1.1. Statistical mechanical Ising surface models*

In order to study surface properties of crystal surfaces, Ising models for the crystal surface are frequently used. In Ising models a crystal is partitioned in cells, and these cells can have only two properties like spin up and spin down or as usual in crystal growth: solid or fluid [1–4]. In Ising surface models the interface crystal–fluid phase is again partitioned in solid and fluid cells and the crystal interface is considered as a gradient in solid and fluid cells going from a complete solid phase with a layer $-\infty$ to a complete fluid phase

with a layer $+\infty$. Within these “gradient-Ising surface models” we will limit ourselves to the one layer model in this paper. In a one layer model the whole interface is reduced to one layer or a “two-dimensional mixed solid–fluid crystal” parallel to the face (hkl).

It has been shown by Onsager in 1944 [5] that in simple two-dimensional crystals an order–disorder phase transition occurs, which may be interpreted as a roughening transition according to Burton, Cabrera and Frank [6,7].

Recently a theory has been developed by Rijpkema et al. [8], which makes it possible to calculate the transition temperatures for any complex planar two dimensional “crystals” where the

blocks are connected to each other by (in principle) first nearest neighbour bonds. In order to determine which faces show an order–disorder phase transition or roughening transition so that they grow with a layer growth mechanism (spiral growth or two-dimensional nucleation) provided of course they grow below this transition temperature we have to determine the two-dimensional crystals where the blocks are connected to each other.

1.2. Crystal graphs

In order to do this we first determine the atoms, ions, molecules or complexes which occur in the mother phase from which the crystal grows. Next we determine the bonds between these species in the crystal structure and in this paper we will limit ourselves as usual to first neighbour bonds only. Next we reduce the atoms, ions, molecules or complexes to “centres of gravity”. In this way the real crystal structure is reduced to a crystal graph, i.e. a set of an infinite number of points with relations (bonds) between these points. The crystal graph fulfils the symmetry of one of the 230 space groups [9]. In practice the space groups corresponds to the space group of the crystal structure under consideration [9,10].

From such a crystal graph the so called two-dimensional connected nets have to be determined. A connected net is a two-dimensional graph, where all the points are connected to each other by paths of bonds. Such a connected net shows an order–disorder phase transition according to the theory of Onsager and its extension to complex crystal structures by Rijpkema [11].

1.3. Crystallographic rules to determine connected nets

The physical principles which determine whether a surface will have an order–disorder phase transition can be translated in crystallographic rules to determine from a crystal graph the connected nets [9,10]. It is shown that in order for a possible connected net to be a real connected net, it is necessary that the whole crystal graph can be unambiguously divided in stacks of equal

connected nets, where the basic structure of these connected nets have no points in common. Furthermore it must be possible to transform the connected nets into themselves and into each other by those symmetry operations or elements of the space group of the crystal graph, which do not change the orientation of the connected net given for example by its reciprocal vector H_{hkl} . It will be shown in forthcoming papers [9,10] and it also will follow from this paper that this implies that for all orientations (hkl) in essence two parallel connected nets, shifted over a distance $\frac{1}{2}d_{nhnknl}$ in reference to each other can be identified. d_{nhnknl} is the interplanar distance corrected for the space group.

1.4. Hartman–Perdok theory

The crystallographic principles to be used in this paper to determine connected nets from a crystal graph go back to the morphological crystallographic theory of Hartman and Perdok [12–15]. In this theory the concept of Periodic Bond Chain (PBC) plays an essential role. A PBC can be defined as an uninterrupted path of bonds to be identified within the crystal graph and having a period $[uvw]$ of the crystal graph.

Two versions of the PBC concept are used nowadays: primitive PBCs and complete PBCs. In the last case to one or more primitive PCSs side branches are added so that a complete PBC is obtained having a stoichiometric composition. Then the whole crystal graph can be partitioned into equal complete PBCs. Complete PBCs consist of one or more cores of primitive PBCs to which a so called periphery of side branches is added [16].

Another concept which plays a key role in the Hartman Perdok theory is the concept of F face. An F face can be defined as a crystallographic face (hkl) parallel to a connected net. Such a connected net is also called F slice [16]. An F slice or connected net consists of at least two different sets of PBCs which are connected to each other. In order to determine connected nets, it is sufficient to check whether primitive PBCs form a connected net. A stack of real connected nets further must fulfill the symmetry rules mentioned above. We note that the Hartman Perdok theory

has been further developed by Strom using graph theory [17], [18]. This makes a computerized determination of connected nets possible [19].

1.5 Determination of growth forms

In order to determine the relative growth rates of different crystallographic forms hkl parallel to connected nets, we will use in this paper the usual E_{hkl}^{slice} and E_{hkl}^{att} [15]. E_{hkl}^{slice} is the energy of a molecule or stoichiometric unit within the connected net under consideration. E_{hkl}^{att} is the energy to remove a stoichiometric unit from its crystallographic position on the connected net and is the complement of E_{hkl}^{slice} given by the relation

$$E^{\text{cr}} = E_{hkl}^{\text{att}} + E_{hkl}^{\text{slice}}, \quad (1)$$

where E^{cr} is the crystallization energy, which is a bulk property independent of the connected net under consideration.

In order to construct growth forms we will assume in this paper that the rate of growth R_{hkl} of a face (hkl) of a crystallographic form $\{hkl\}$ is proportional to E_{hkl}^{att} . Although a parallel relation between E_{hkl}^{att} and R_{hkl} (in the sense that for two faces the relation holds: if $E_1^{\text{att}} > E_2^{\text{att}}$ then $R_1 > R_2$) can be strongly justified from crystal growth theories [20], a strict proportionality cannot be derived logically from these theories. Yet using this proportionality growth forms can be predicted which are in good agreement with observed growth forms [21,22].

1.6. Bond energies at the surface

We note that for the crystal–fluid interface, within the frame work of Ising models bond energies have the usual form:

$$\phi = \phi^{\text{sf}} - \frac{1}{2}(\phi^{\text{ss}} + \phi^{\text{ff}}), \quad (2)$$

where s and f refer to solid and fluid respectively and the corresponding bonds to solid–fluid bonds, etc. The ff and sf bond energies are not known, but in the following we will assume as usual that ϕ^{ss} bond energies are proportional to the bond energies. This assumption has led to good results for, for example, garnets [16].

1.7. Aim of the paper

It is the aim of this paper to apply the crystallographic principles, which result from the statistical mechanical theories of roughening transition and order–disorder phase transition in two-dimensional connected nets, to the complex crystal structure of apatite. This is the most important phosphate mineral and a lot of morphological data are known. In biology this crystal structure plays a key role in teeth and bones.

In another paper we applied the extended statistical mechanical Onsager [5] theory by Rijpkema et al. [8] to the connected nets of apatite determined in this paper [23]. The simplified structure of some connected nets will also be shown in ref. [23].

2. Apatite structure

2.1. Chemical composition of apatites

The general formula for the group of minerals called apatite is $\text{Me}_{10}(\text{AO}_4)_6\text{X}_2$. In this paper, although not essential, we use $\text{Me} = \text{Ca}$, $\text{A} = \text{P}$ and $\text{X} = \text{OH}$ so that we get what is often called the prototype of the mineral in bone and teeth; $\text{Ca}_{10}(\text{PO}_4)_6(\text{OH})_2$, hydroxyapatite. Other substitutions that are known to occur in these mineralized tissues are $\text{Me} = \text{Na}$, K and possibly Mg , $\text{AO}_4 = \text{CO}_3$, $\text{X} = \frac{1}{2} \text{CO}_3$ (tooth enamel), F , Cl .

In apatites occurring in nature and in synthetic apatites, numerous substitutions are known to occur. Apatite got its name meaning “to cheat” because it was often confused with other minerals [25].

2.2. Structure and space group of apatites

The crystal structure of hydroxyapatite has been determined by Posner et al. [26] and was refined by Kay et al. [27]. The apatite structure can be described as a distorted hexagonal closest packing of AO_4 “spheres”. The cations occupy two different sites. One (Ca I at $\frac{1}{3}, \frac{2}{3}, Z$) is an octahedral site, occupied for 2/3 by cations, so in between the planes of AO_4 “spheres” along the main axis.

The X-ions are situated on the main axis and the space group depends on the position and orientation of the X-ions. For $X = F$, the F is in the AO_4 plane and the space group is $P6_3/m$.

In $X = Cl$, the Cl is out of the AO_4 plane, ordering of the Cl in a column (on the main axis) and ordering of the columns results in the monoclinic space group $P2_1/b$ [28].

In $X = OH$, the OH is not exactly in the AO_4 plane, its axis is parallel to the main axis and the orientation of the OH can either be random – then the space group is $P6_3/m$ – or ordered in a column (rows of OH ions are formed) and then the ordering of these columns results in the monoclinic space group $P2_1/b$ [28].

2.3. Types of bonds in hydroxyapatite

Only the bonds that are formed during the crystallization process are relevant for the morphological analysis, and only first nearest neighbour interactions are considered, but this approximation gives good results as has been shown amongst other for garnet [16] and as will also appear from this paper.

For the analysis the crystal structure is simplified to centres of gravity representing the growth units. These are interconnected and form a crystal graph. The interconnections represent first nearest neighbour bonds.

The types of bonds that are relevant then are 6 different Ca– PO_4 bonds and one Ca–OH bond.

The energy of these bonds can be calculated on the basis of coulombic interaction. The charge on each PO_4^{3-} oxygen is taken to be $-1.048e$ and on the phosphorus $+1.192e$ according to ref. [29]. The charge on the oxygen of OH^- is taken to be $-2e$. It is found then, using the coordinates of ref. [26], that the energies of the 6 different Ca– PO_4 bonds are very close to each other and lie within the range of $2431 \text{ kJ/mol} \pm 6\%$. The Ca–OH bond energy is 1269 kJ/mol .

For the calculation of the slice energy we will assume the Ca– PO_4 bonds to be equally strong and the Ca–OH bond will be taken half as strong as the Ca– PO_4 bonds.

In fig. 3 a projection along the $[001]$ direction of hydroxyapatite is shown. The different types of

bonds are shown, as well as the z coordinate of the ions.

3. Application of the Hartman–Perdok theory [2–5] to apatite

3.1. Geometrical criterion to search for the most important PBC directions

According to the Hartman–Perdok theory, the morphology of a crystal is governed by uninterrupted chains of strong bonds running through the structure and having a period $[uvw]$ of the lattice. Such a chain of strong bonds is called a complete periodic bond chain (PBC). Only strong bonds that are formed during the crystallization process are relevant.

Complete PBCs have the stoichiometry of the crystal structure, and it is expected that the shortest translation distances are potential PBC directions.

Table 1 shows the PBC directions and the length of their period which resulted from an investigation of the shortest translation distances. It is interesting to note that Amelinckx [30] has found growth spirals on $\{10\bar{1}0\}$ which are parallel to $\langle 001 \rangle$, $\langle 100 \rangle$ and $\langle 101 \rangle$.

3.2. Geometrical criterion for the search for F slices

The morphological importance of a crystal form $\{hkl\}$ is a relative statistical measure for the

Table 1

The PBC directions used in this study to search for potential F slices and the length of one translation expressed in $a_0 = 9.42 \text{ \AA}$

PBC	Length of one translation in PBC direction (a_0)
$\langle 001 \rangle$	0.73
$\langle 100 \rangle$	1
$\langle 101 \rangle$	1.24
$\langle 1\bar{1}0 \rangle$	1.73
$\langle 120 \rangle$	1.87
$\langle 121 \rangle$	1.98
$\langle 122 \rangle$	2.27
$\langle 120 \rangle, \langle \bar{2}10 \rangle$	2.64

3.3. Survey of potential F slices or connected nets using a stereographic projection

When the circles of zones that are parallel to one of the PBC directions from table 1 are drawn in a stereogram the points of intersection represent faces that are parallel to two or more PBC directions and so they are potential F faces (fig. 1). These potential F faces from the stereographic projection are examined in one or more of the projections in a PBC direction further on. Anticipating our analysis, it can be shown that only the points of intersection that have been marked are real F faces.

All the faces that have been marked belong to different forms, equivalent faces can be obtained by applying the symmetry of the point group $6/m$.

For comparison with table 1 it should be noted that $\langle 121 \rangle \equiv [121]$ and equivalents, $\langle 122 \rangle \equiv [122]$ and equivalents, etc.

3.4. Procedure to determine F slices or connected nets

The approach was to examine the potential F faces from the stereogram in the appropriate projections in different PBC directions, and to this end the criteria developed for the determination of connected nets of ref. [9], and which have been mentioned in sections 1.2 and 1.4 already, were used. Connected nets run parallel to F faces and they are called F slices [9].

For the determination of the connected nets and so of the F slices, the PBCs need not be stoichiometric, as was required by the actual definition [12–15]. We recall that these criteria for the determination of the connected nets were the following: (i) the whole crystallograph must be partitioned into independent basic connected nets and (ii) the set of basic connected nets must be invariant under those symmetry operations or symmetry elements which leave the direction of the reciprocal vector H_{nhnknl} perpendicular to the F slice ($nhnknl$), invariant.

In the present study it was realized that criterion (ii) implies that the symmetry elements meant above can only be situated exactly in the border of

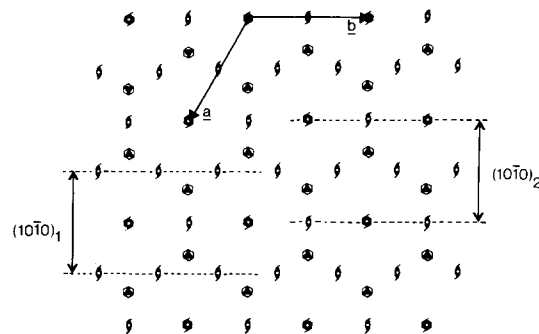


Fig. 2. Projection in $[001]$ direction showing the two $(10\bar{1}0)$ alternatives relative to the position of the twofold screw axes and centres of symmetry. Of the six fold screw axis (6_3) only the sub-group 2_1 is relevant. The sixfold inversion axis is not relevant in the sense of the second criterion of ref. [9].

a slice or exactly in the middle of a slice. This means that always only two alternative F slices ($nhnknl$) are possible, shifted $\frac{1}{2}d_{nhnknl}$ in reference to each other.

This principle is illustrated for the two potential F slices $(10\bar{1}0)_{1,2}$ seen edge on the $[001]$ projection (fig. 2) where now only the symmetry elements are shown. It should be noted that $\bar{6}$ and 6_3 are not relevant in the sense of criterion (ii), but only 2_1 as a subgroup of 6_3 is relevant here.

It can be seen from fig. 2 that indeed only two alternative potential F slices $(10\bar{1}0)_{1,2}$ can be drawn, of which the border lines are not necessarily straight. The relevant symmetry elements, however, have to be located exactly at the border or in the middle of the slice, otherwise criterion (ii) will be violated and then the slice cannot represent a real connect net.

We note that so far we only have partitioned the space of a crystal graph in “empty” slices. It cannot be predicted whether the two alternative “space slices” will always be “filled” with two alternative connected nets. This depends on the actual crystallograph. In this connection it is interesting to mention that in case of garnet of the six F faces alternatives for $\{400\}$ and $\{420\}$ were absent [16]. If slices become sufficiently thin both alternative empty slices cannot be filled with connected nets. It has to be noted that although in principle only two alternative F slices ($nhnknl$) are possible, for each alternative slice more alternatives may be found by attaching and detaching

different point of the graph in the boundary to the F slice.

But as soon as assumptions have been made about the relative bond strength in the crystal, it will be clear how the border line of a slice has to be drawn and what the position of an atom (at the border) in the slice has to be, to make the slice (connected net) as strong as possible.

3.5. Labeling of PBCs and slices

The PBCs are labelled with the symbol $[uvw]_{xy}$, where uvw indicates the period of the PBC, x is used to distinguish between different PBCs with equal $[uvw]$ and y to distinguish between equal PBCs in different slices.

The F slices are labelled $(nhnkn)_z$ where h , k and l are Miller indices of the corresponding F face and n depends on the presence of (pseudo-) symmetry operations affecting the slice thickness. z equals 1 or 2 in case of two alternative F slices; in the absence of an alternative slice, z is not relevant.

In the projections in the four PBC directions, the PBCs that are drawn are seen end on. In some of the projections some non-equivalent atoms overlap and this can be recognized when in the projection one atom (in fact two overlapping non-equivalent atoms) seems to belong to two different PBCs in one slice or in different slices. But in this case always one atom belongs to only one PBC. (In figs. 3–6, the points enclosed by solid lines correspond to (primitive) PBCs. The PBCs within the borders of the slices (dashed lines) are interconnected and together they form a connected net.)

4. Projections in four different PBC directions

4.1. Projection in $[001]$ direction

It can be seen from fig. 3 that nine PBCs $[001]_{xy}$ can be identified in the projection in the $[001]$ direction. These occur in six different F

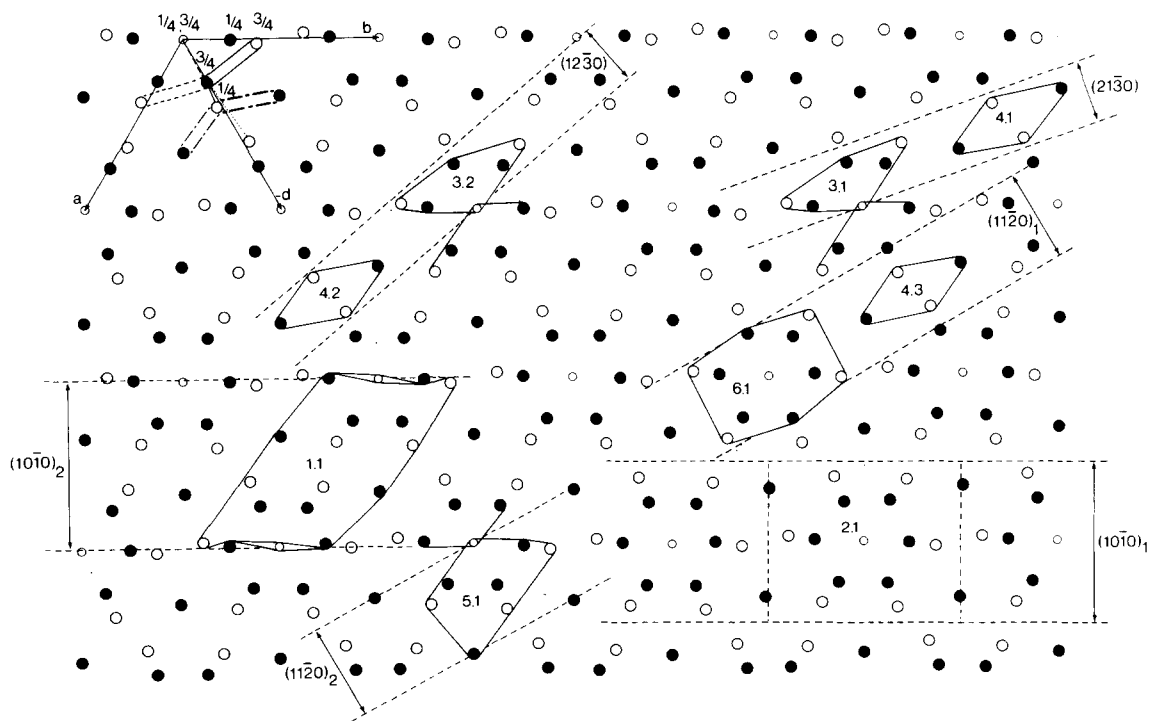


Fig. 3. Projection in $[001]$ direction. See section 4.1. Solid circle is Ca. Large open circle is PO_4 , small open circle is OH. The points enclosed by solid lines correspond to (primitive) PBCs, seen end on.

slices. These slices are the following (xy of the PBCs $[001]_{xy}$ occurring in the slice will be given between brackets): $(10\bar{1}0)_2$ (1.1), $(10\bar{1}0)_1$ (2.1), $(21\bar{3}0)$ (3.1, 4.1), $(12\bar{3}0)$ (4.2, 3.2), $(11\bar{2}0)_2$ (5.1), $(11\bar{2}0)_1$ (6.1, 4.3). The slices $(21\bar{3}0)$ and $(12\bar{3}0)$ are two slices with equal PBCs but with different bonds between those PBCs. The slices $(10\bar{1}0)_{1,2}$ and the slices $(11\bar{2}0)_{1,2}$ are shifted $\frac{1}{2}d_{10\bar{1}0}$ respectively $\frac{1}{2}d_{11\bar{2}0}$ reference to each other.

4.2. Projection in the $[100]$ direction

It can be seen from fig. 4 that ten PBCs $[100]_{xy}$ from nine F slices of which seven are new. These slices are the following (xy of the PBCs $[100]_{xy}$ occurring in the slice is given between brackets): $(02\bar{2}1)_1$ (1.1), $(02\bar{2}1)_2$ (2.1), (0002) (3.1), $(01\bar{1}0)_2$ (4.1), $(01\bar{1}0)_1$ (3.2), $(01\bar{1}2)$ (5.1), $(01\bar{1}1)_1$ (6.1), $(01\bar{1}1)_2$ (7.1), $(02\bar{2}2)$ (8.1, 9.1).

The slices $(02\bar{2}1)_{1,2}$, $(01\bar{1}0)_{1,2}$ and $(01\bar{1}1)_{1,2}$ are

shifted respectively $\frac{1}{2}d_{02\bar{2}1}$, $\frac{1}{2}d_{01\bar{1}0}$ and $\frac{1}{2}d_{01\bar{1}1}$ in reference to each other. For the slices $(01\bar{1}1)_{1,2}$ it is also possible to determine F slices with thickness $\frac{1}{2}d_{01\bar{1}1}$. Two slices $(02\bar{2}2)_{A,B}$ are formed which are related through a centre of symmetry and the slice energy E^{slice} of slice A and B is exactly the same. Both slices however expose a different surface to the solution, so that the attachment energy E^{att} and the growth kinetics will in principle be different (see also ref. [35] where this problem is treated).

If E^{att} and the growth kinetics are very different for the two slices A and B, one of the two surfaces will be energetically favoured and growth will occur in layers with thickness $d_{01\bar{1}1}$.

If E^{att} and the growth kinetics of the two slices A and B are similar then growth will occur in layers with thickness $d_{02\bar{2}2}$.

The slice energy E^{slice} which we will use to predict the morphological importance (MI) of the

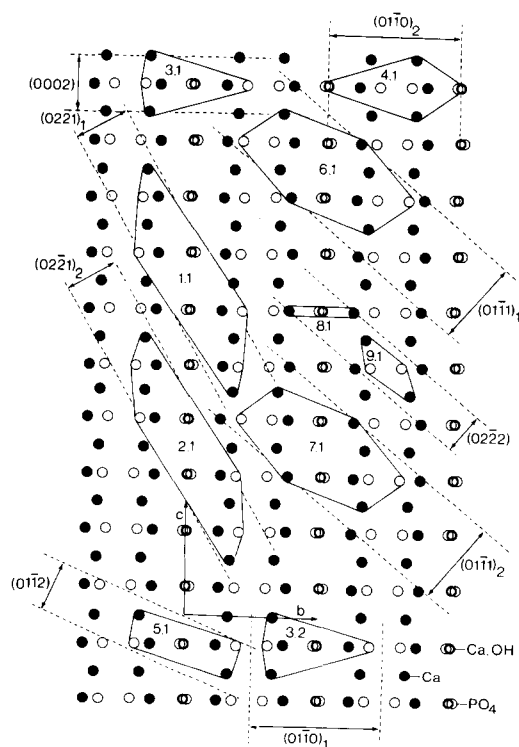


Fig. 4. Projection in $[100]$ direction. See section 4.2. Symbols as in fig. 3.

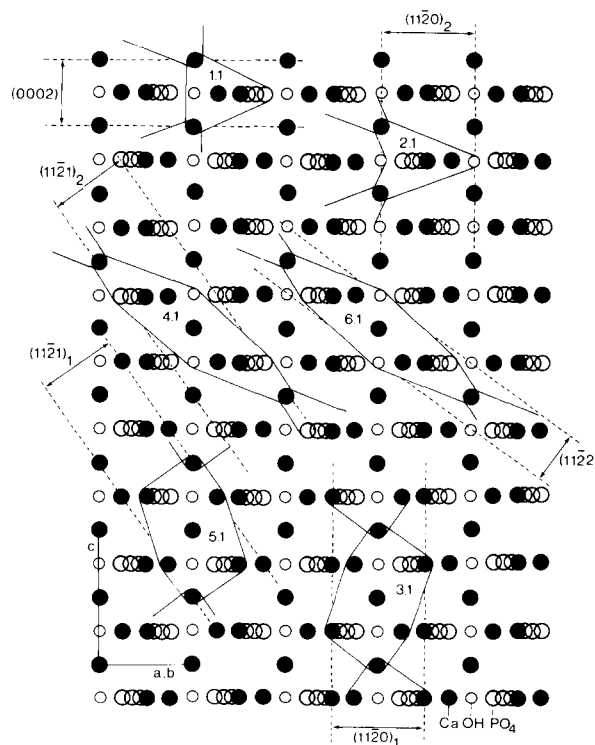


Fig. 5. Projection in $[1\bar{1}0]$ direction. See section 4.3. Symbols as in fig. 3.

F slices will be smaller for the slices $(02\bar{2}2)_{A,B}$ than for $(01\bar{1}1)_{1,2}$ and so there will be a difference in the predicted morphological importance.

From the best agreement between the predicted MI on the basis of E^{slice} and the observed MI of the slices concerned it will eventually be clear what will be the thickness of the growth layer.

It should be noted that in case of two alternative slices with equal d_{hkl} which are shifted $\frac{1}{2}d_{hkl}$ in reference to each other, the slice with the higher slice energy will determine the predicted MI.

4.3. Projection in the $[1\bar{1}0]$ direction

It can be seen in fig. 5 that six PBCs $[1\bar{1}0]_{xy}$ from six F slices of which three are new ones. These slices are the following (xy of the PBCs $[1\bar{1}0]_{xy}$ is given between brackets): (0002) (1.1), $(11\bar{2}0)_2$ (2.1), $(11\bar{2}0)_1$ (3.1), $(11\bar{2}1)_2$ (4.1), $(11\bar{2}1)_1$

(5.1) , $(11\bar{2}2)$ (6.1). The F slices (0002) , $(11\bar{2}0)_2$ and $(11\bar{2}0)_1$ had already been determined. The slices $(11\bar{2}1)_{1,2}$ and $(11\bar{2}0)_{1,2}$ are shifted $\frac{1}{2}d_{11\bar{2}1}$ respectively $\frac{1}{2}d_{11\bar{2}0}$ in reference to each other.

4.4. Projection in the $[01\bar{1}]$ and $[10\bar{1}]$ direction

It can be seen from fig. 6 that eight PBCs $[01\bar{1}]_{xy}$ form eight F slices. These slices are the following (xy of the PBCs $[01\bar{1}]_{xy}$ is given between brackets): $(12\bar{1}2)$ (1.1), $(10\bar{1}0)_1$ (2.1), $(10\bar{1}0)_2$ (3.1), $(01\bar{1}1)_1$ (2.2), $(01\bar{1}1)_2$ (4.1), $(11\bar{2}1)_1$ (5.1), $(11\bar{2}1)_2$ (6.1), $(21\bar{3}1)$ (7.1).

The slices $(10\bar{1}0)_{1,2}$, the slices $(01\bar{1}1)_{1,2}$ and the slices $(11\bar{2}1)_{1,2}$ are shifted respectively $\frac{1}{2}d_{10\bar{1}0}$, $\frac{1}{2}d_{01\bar{1}1}$ and $\frac{1}{2}d_{11\bar{2}1}$ in reference to each other. The slice $(21\bar{3}1)$ is the only slice in this projection which had not been determined yet.

In the insert in fig. 6 it can be seen that in the projection in the $[10\bar{1}]$ direction one new F slice $(12\bar{3}1)$ is determined.

5. Calculation of E_{hkl}^{slice}

E_{hkl}^{slice} is the total energy of all bonds in a slice per stoichiometric unit and it can be used as a measure for the morphological importance of a slice (hkl) [20]. In table 3 E_{hkl}^{slice} is given for the F slices found in this study and the MI order which follows from E_{hkl}^{slice} is compared with the observed MI.

For the relative bond strengths we have assumed that all Ca- PO_4 bonds are equally strong and that the ratio of such a mean Ca- PO_4 bond and a Ca-OH bond is $\Phi^{\text{Ca-PO}_4} : \Phi^{\text{Ca-OH}} = 2 : 1$ (see also section 2.3).

E_{hkl}^{slice} is expressed in $\Phi^{\text{Ca-PO}_4}/\text{cell}$ contents. In table 3, also the attachment energy E_{hkl}^{att} is given, which is related to E_{hkl}^{slice} through eq. 91) (see section 1.5):

$$E^{\text{cr}} = E_{hkl}^{\text{att}} + E_{hkl}^{\text{slice}}.$$

E^{cr} is a bulk property and the same for each slice. For hydroxyapatite E^{cr} equals 57 ($\Phi^{\text{Ca-PO}_4}/\text{cell}$ contents) and is constituted from 54 Ca- PO_4 bonds and 6 Ca-OH bonds.

In order to find out the importance of the

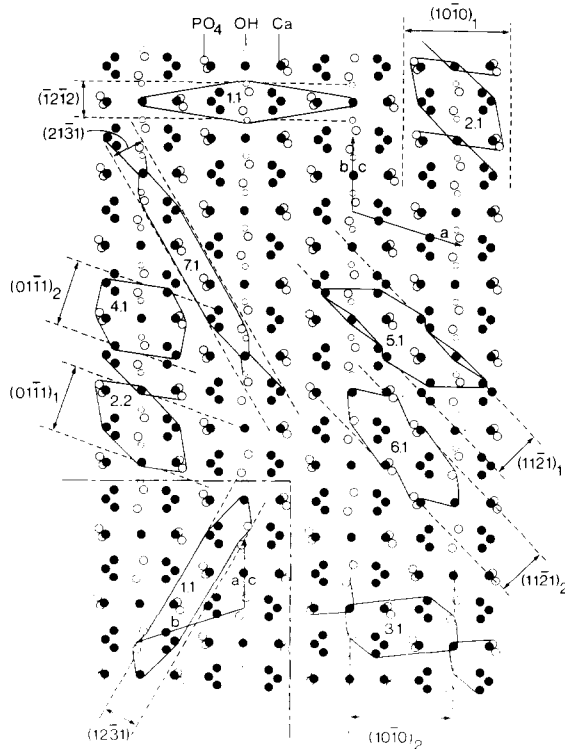


Fig. 6. Projection in $[01\bar{1}]$ and $[10\bar{1}]$ directions. See section 4.4. Symbols as in fig. 3.

Table 3
 E_{hkl}^{slice} and E_{hkl}^{att} calculated for all connected nets determined in this study

Connected net (<i>hkl</i>)	Number of bonds of type		E_{hkl}^{slice} (Φ^{Ca-PO_4})	E_{hkl}^{att} (Φ^{Ca-PO_4})	MI, predicted order	E_{hkl}^{slice} (for $\Phi^{Ca-OH} = 0$)	MI, predicted order	MI, observed order (%)
	Ca-PO ₄	Ca-OH						
(10 $\bar{1}$ 0) ₁	42	6	45	12	1	42	1	1 (97)
(10 $\bar{1}$ 0) ₂	42	4	44	13	—	42		
(01 $\bar{1}$ 1) ₁	36	6	39	18	2	36	2	3/4 (72)
(01 $\bar{1}$ 1) ₂	36	6	39	18		36		
(11 $\bar{2}$ 0) ₂	36	4	38	19	3	36	3	5 (64)
(11 $\bar{2}$ 0) ₁	32	6	35	22	—	32	—	
(0002)	30	6	33	24	4	30	4	2 (89)
(11 $\bar{2}$ 1) ₁	28	6	31	26	5	28	5	3/4 (72)
(11 $\bar{2}$ 1) ₂	28	4	30	27	—	28		
(02 $\bar{2}$ 1) ₁	26	4	28	29	6/7/8	26	6/7/8	6 (59)
(02 $\bar{2}$ 1) ₂	26	4	28	29		26		
(21 $\bar{3}$ 0)	26	4	28	29	6/7/8	26	6/7/8	11/(11)
(12 $\bar{3}$ 0)	26	4	28	29	6/7/8	26	6/7/8	11/(11)
(02 $\bar{2}$ 2)	24	6	27	30	9	24	9/10	Comp. (01 $\bar{1}$ 1) _{1,2}
(01 $\bar{1}$ 2)	23	6	26	31	10/11	23	11	7 (54)
(11 $\bar{2}$ 2)	24	4	26	31	10/11	24	9/10	9 (23)
(21 $\bar{3}$ 1)	21	4	23	34	12/13	21	12/13	8/(40)
(12 $\bar{3}$ 1)	21	4	23	34	12/13	21	12/13	8/(40)

Ca-OH bond for the morphology of apatite, we have also calculated E_{hkl}^{slice} for the hypothetical case where $\Phi^{Ca-OH} = 0$ (see table 3).

6. Conclusion and discussion

The prediction of the order of morphological importance by E_{hkl}^{slice} is in good agreement with the observed MI. From the much better agreement between the predicted and the observed MI of (01 $\bar{1}$ 1)_{1,2} compared to (02 $\bar{2}$ 2), we concluded that the growth layer thickness will be $d_{01\bar{1}1}$.

Furthermore we note that the Ca-OH bond has no influence on the order of the morphological importance (table 3). Taking this bond as zero does also not change the character of any of the F faces which have been determined. This is an interesting result in the light of a suggestion about the possible cause for the low symmetry of biological apatitic crystals (generally these have a plate-like habit) by Elliott et al. [28]. As has been referred to in this paper already, Elliott et al. suggest that the low symmetry might be due to the ordering of OH and OH columns which results in

a lowering of the symmetry of the space group from P6₃/m to P2₁/b.

If this ordering of OH has any influence on the Ca-OH bonds at all, it will not be significant and there will still be a pseudo symmetry P6₃/m, so that we expect monoclinic hydroxyapatite to have the same morphological appearance as hexagonal hydroxyapatite.

The possible involvement of another calcium phosphate, i.e. octacalcium phosphate, in the occurrence of plate-like apatitic crystals in biological systems (teeth and bones) as suggested by Brown (see ref. [37]) will be discussed in a further study [38].

Acknowledgements

One of the authors (R.A. Terpstra) was supported by HGO/TNO (project No. 13-52-19). The authors thank S.M. Wolfrum for assisting in the use of the computer plotting program PLUTO [36]. Dr. J. van der Eerden and Professor F.C.M. Driessens are thanked for useful discussions and suggestions.

References

- [1] D.E. Temkin, in: *Crystallization Processes* (Consultants Bureau, New York, 1966) p. 15.
- [2] P. Bennema and G.H. Gilmer, in: *Crystal Growth: An Introduction*, Ed. P. Hartman (North-Holland, Amsterdam, 1973) p. 263.
- [3] G.H. Gilmer and P. Bennema, *J. Appl. Phys.* 43 (1972), 1347.
- [4] J.P. van der Eerden, P. Bennema and T.A. Cherepanova, in: *Progress in Crystal Growth and Characterization*, Vol. 1, Ed. B. Pamplin (Pergamon, Oxford, 1978) p. 219.
- [5] L. Onsager, *Phys. Rev.* 65 (1944) 117.
- [6] W.K. Burton, N. Cabrera and F.C. Frank, *Phil. Trans. Roy. Soc. London A243* (1951) 299.
- [7] P. Bennema, *J. Crystal Growth* 69 (1984), 182.
- [8] J.J.M. Rijpkema, H.J.F. Knops, P. Bennema and J.P. van der Eerden, *J. Crystal Growth* 61 (1982) 295.
- [9] P. Bennema and J.P. van der Eerden, *Crystal graphs, connected nets, roughening transition and the morphology of crystals*, in a book on morphology, Ed. I. Sunagawa, to be published.
- [10] P. Bennema, *Crystallographic rules to determine connected nets from crystal graphs based on the theory of roughening transition*, in: *Proc. Oji Seminar*, Aug. 1985, Japan, Ed. I. Sunagawa, to be published.
- [11] J.J.M. Rijpkema, Thesis, University of Nijmegen (1984).
- [12] P. Hartman, W.G. Perdok, *Acta Cryst.* 8 (1955) 49.
- [13] P. Hartman, W.G. Perdok, *Acta Cryst.* 8 (1955) 521.
- [14] P. Hartman, W.G. Perdok, *Acta Cryst.* 8 (1955) 525.
- [15] P. Hartman, *Structure and Morphology in: Crystal Growth: An Introduction*, Ed. P. Hartman (North-Holland, Amsterdam, 1973) p. 367.
- [16] P. Bennema, E.A. Giess and J.E. Weidenborner, *J. Crystal Growth* 62, (1983) 41.
- [17] C.S. Strom, *Z. Krist.* 153 (1980) 99.
- [18] C.S. Strom, *Z. Krist.* 154 (1981) 31.
- [19] C.S. Strom, *Z. Krist.* 172 (1985) 11.
- [20] P. Hartman and P. Bennema, *J. Crystal Growth* 49 (1980) 145.
- [21] J. 't Hart, Thesis, State University Leiden (1978).
- [22] I. Weissbuch, L. Addadi, Z. Berkovitch-Yellin, E. Gati, S. Weinstein, M. Lahar and L. Leiserowitz, *J. Am. Chem. Soc.* 105 (1983) 6615.
- [23] R.A. Terpstra, J.J.M. Rijpkema and P. Bennema, *J. Crystal Growth* 76 (1986) 494.
- [24] L.A.M.J. Jetten, H.J. Human, P. Bennema and J.P. van der Eerden, *J. Crystal Growth* 68 (1984) 503.
- [25] G.A. Werner, *Bergmann Journal* 1 (1788) 77.
- [26] A.S. Posner, A. Perloff and A.F. Diorio, *Acta Cryst.* 11 (1958) 308.
- [27] M.I. Kay, R.A. Young and A.S. Posner, *Nature* 204 (1964) 1050.
- [28] J.C. Elliott, P.E. Mackie and R.A. Young, *Science* 180 (1973) 1055.
- [29] H. Johansen, *Theoret. Chim. Acta* 32 (1974) 273.
- [30] S. Amelinckx, *Nature* 170 (1952) 760.
- [31] G. Friedel, *Bull. Soc. Franc. Minéral.* 30 (1907) 326.
- [32] J.D.H. Donnay and D. Harker, *Am. Mineralogist* 22 (1937) 446.
- [33] J.D.H. Donnay and G. Donnay, *Comp. Rend. (Paris)* 252 (1961) 908.
- [34] V. Goldschmidt, *Atlas der Kristallformen*, Band, 2 (Winters, Heidelberg, 1913).
- [35] W.M.M. Heijnen, Thesis, University of Utrecht (1986), ch. II. to be published.
- [36] W.D.S. Motherwell and W. Clegg, *PLUTO program for the production of crystal and molecular illustrations* (Cambridge Crystallographic Data Centre, Cambridge, UK, 1978).
- [37] W.E. Brown, M. Mathew and M.S. Tung, *Progr. Crystal Growth Characterization* 4 (1981) 59.
- [38] R.A. Terpstra and P. Bennema, *J. Crystal Growth*, to be published.